BEST AVAILABLE IMAGES

Defective images within this document are accurate representations of the original documents submitted by the applicant.

Defects in the images may include (but are not limited to):

- BLACK BORDERS
- TEXT CUT OFF AT TOP, BOTTOM OR SIDES
- FADED TEXT
- ILLEGIBLE TEXT
- SKEWED/SLANTED IMAGES
- COLORED PHOTOS
- BLACK OR VERY BLACK AND WHITE DARK PHOTOS
- GRAY SCALE DOCUMENTS

IMAGES ARE BEST AVAILABLE COPY.

As rescanning documents *will not* correct images, please do not report the images to the Image Problem Mailbox.

PCT/AU00/00004

Patent Office
Canberra

4

I, ANNA MAIJA MADL, ACTING TEAM LEADER EXAMINATION SUPPORT & SALES hereby certify that annexed is a true copy of the Provisional specification in connection with Application No. PQ 3938 for a patent by MEDITECH RESEARCH LIMITED filed on 09 November 1999.

WITNESS my hand this
Eighteenth day of February 2000

A.M. Madl

ANNA MAIJA MADL
ACTING TEAM LEADER
EXAMINATION SUPPORT & SALES

PRIORITY DOCUMENT
SUBMITTED OR TRANSMITTED IN COMPLIANCE WITH RULE 17.1(a) OR (b)

AUSTRALIA

Patents Act 1990

PROVISIONAL SPECIFICATION

Applicant(s):

MEDITECH RESEARCH LIMITED

A.C.N. 058 390 953

Invention Title:

A COMPOSITION AND METHOD FOR THE ENHANCEMENT OF THE EFFICACY OF DRUGS

The invention is described in the following statement:

of the cancer cells to the active compound is often observed. Moreover, it is often found that resistance to one drug may confer resistance to other biochemically distinct drugs. This has been termed multidrug resistance. Drugs that are typically affected by the multidrug resistance problem include doxorubicin, vincristine, vinblastine, colchicine and actinomycin D. In at least some cases, multidrug resistance is a complex phenotype that has been linked to a high level of expression of a cell membrane drug efflux transporter called MdrI protein, also known as P-glycoprotein. This membrane "pump" has broad specificity, and acts to remove from the cell a wide variety of chemically unrelated toxins (see Endicott et al., 1989).

Recently, a similar mechanism of broad-spectrum drug resistance has been reported for certain microorganisms. These results indicate the existence of bacterial efflux systems of extremely broad substrate specificity that are similar to the multidrug resistance pump of mammalian cells (see Nikaido, 1993).

Substances which reverse multidrug resistance are known as resistance modification agents (RMAs), and are of importance in potentiating the cytotoxicity of chemotherapeutic agents to which a human cancer has become resistant. Although many agents have been identified as RMAs *in vitro*, a large proportion of these have little or no therapeutic potential because of high toxicity *in vivo* at the doses required to reverse multidrug resistance. For example, metabolic poisons, such as azide, are able to reverse multidrug resistance *in vitro*, but have no usefulness *in vivo*. Most other highly effective RMAs, such as PSC833, appear to work as competitive antagonists of a drug-binding site on the MdrI protein. Many of these agents also have toxicity that limits their usefulness *in vivo*. Consequently, there is a need to develop alternate pharmacological strategies for reversing multidrug resistance.

because methotrexate is relatively insoluble in water; therefore if this were to occur it would be a very weak interaction. The most likely bonding between MTX and HA would be via hydrophobic interactions between MTX's numerous hydrophobic groups and the hydrophobic patches in the secondary structure of HA (Scott et al., 1989).

(ii) *Molecular Association.*

Where MTX is merely "mixed" in HA gel (Figure 2B) with no specific chemical bond formation, MTX could become entrapped within the 3-dimensional meshwork formed by higher concentrations of HA (Mikelsaar and Scott, 1994), so that the drug simply diffuses from the HA after administration. If HA is rapidly taken up and bound by specific cell receptors, the drug will be released in higher concentration at these points eg. lymph nodes, liver, bone marrow, tumour cells with HA receptors.

While again not wishing to be bound by any particular theory, one mechanism by which HA helps to target active agents may be via the characteristic over-expression of HA receptors in several tumour types (Stamenkovic *et al.*, 1991; Wang *et al.*, 1998). The HA receptors CD44, Receptor for Hyaluronan Mediated Motility (RHAMM) and ICAM-1, have been linked to tumour genesis (Bartolazzi *et al.*, 1994) and progression (Günthert 1993; Arch *et al.*, 1992). RHAMM is a major factor in mediating tumour cell motility and invasion (Hardwick *et al.*, 1992). It has been demonstrated that RHAMM is required for H-ras transformation of fibroblasts (Hall *et al.*, 1995), which would make this receptor a potential participant in tumour formation and growth. ICAM-1, a receptor tentatively linked to HA metabolism (McCourt *et al.*, 1994), is highly expressed in transformed tissues such as mouse mastocytomas (Gustafson *et al.*, 1995) and in the stroma and clusters of tumour cells of human breast carcinomas (Ogawa *et al.*, 1995).

Increased expression of HA receptors on tumour cells provides a rationale for attempting the incorporation

effectiveness of a drug, comprising the step of administration of a pharmaceutical composition comprising hyaluronan and said drug.

While not wishing to be bound by theory, it is believed possible mechanisms for overcoming drug resistance are:

1. Hyaluronan binds to receptors on the resistant cell or enters the cell via bulk endocytosis, resulting in the entrained or bound drug being delivered into the cell, allowing it to become therapeutically active.

2. Hyaluronan binds to the surface of the resistant cell, where the entrained or bound drug diffuses from the hyaluronan meshwork into the cell, resulting in the drug being delivered to the resistant cell.

3. Hyaluronan and other mucopolysaccharides adopt a coiled configuration that entrains the drug, and may also bind a variety of drugs.

Accordingly in a fourth aspect, the present invention provides a method of overcoming drug resistance, comprising the step of co-administering a drug with a mucopolysaccharide capable of entraining and/or binding said drug and capable of binding to receptors on the resistant cell or entering the cell via bulk endocytosis, wherein said drug is delivered into the cell, thereby allowing it to become therapeutically active.

According to a fifth aspect of the present invention there is provided a method of overcoming or reducing drug resistance, comprising the step of co-administering a drug and a mucopolysaccharide capable of entraining and/or binding said drug and capable of binding to the surface of the resistant cell, wherein the entrained or bound drug diffuses from said mucopolysaccharide into the cell.

While not wishing to be bound by theory, it may also be that a combination of hyaluronan with a drug results in the drug being retained in the cell for a longer period, allowing a prolonged release and more time for the

co-administering a drug and a mucopolysaccharide capable of entraining or binding said drug and/or associating with said drug in such a manner that said drug has reduced gastrointestinal toxicity.

Throughout the description and claims of this specification, the word "comprise" and variations of the word, such as "comprising" and "comprises", means "including but not limited to" and is not intended to exclude other additives, components, integers or steps.

BRIEF DESCRIPTION OF THE FIGURES

Figure 1 shows that in higher concentrations HA forms a three-dimensional meshwork which is capable of entraining small molecules such as methotrexate. The HA/drug targeting of pathological sites is accomplished by the HA rapidly binding to specific cell receptors, followed by diffusion of the drug from the HA, and/or co-internalization of both the HA and drug via HA and/or drug receptors.

Figure 2A shows the possible molecular interactions between methotrexate and HA. These include (i) ionic bonding, (ii) hydrogen bonding or (iii) hydrophobic bonding.

Figure 2B is a diagrammatic representation of the entanglement of methotrexate in HA. At higher concentrations HA forms a 3-dimensional meshwork which is represented by the large coiled molecule. (*) represents the methotrexate which has a molecular weight of only 454D, and is easily entrained in the 400-900 kD HA molecule.

Figure 3 shows the general pathology of human breast cancer tumours grown in nude mice. Panel A shows the general morphology of a grade II-III human tumour. Panel B shows a micrograph of another section of the tumour exhibited in Figure 3A. This section shows the surrounding mouse muscle (M), tumour capsule (C), necrotic areas of the tumour (N), infiltrating tumour (T) and (→) indicates a common phenomenon known as "Indian files", in which

Figure 11 shows the cytotoxic synergistic in vitro effect of combining HA with 5-FU.

Figure 12 shows 5-FU targeting of human breast cancer tumours using HA as a carrier.

Figure 13 shows elimination pathways of HA in humans.

Figure 14 shows increased uptake of 5-FU in the stomach, brain and lungs.

Figure 15 shows the effect of HA on the pharmacokinetics elimination of plasma 5-FU.

Figure 16 shows the criteria for definition of experimental end-point. Criteria 2 (Panel A) and Criteria 3 (Panel B) are shown.

Figure 17 shows the efficacy of 5-FU/HA adjuvant therapy (6 week treatment regimen): Effect on primary tumour volume.

Figure 18 shows the efficacy of 5-FU/HA adjuvant therapy (6 week treatment regimen): Effect on body mass.

Figure 19 shows the efficacy of 5-FU/HA adjuvant therapy (6 week treatment regimen): Effect on spread of cancer lymph nodes and formation of new tumours.

Figure 20 shows the general appearance of tumours of the 6 month efficacy study.

Figure 21 shows the effect of HA/5-FU adjuvant therapy on patient survival.

ABBREVIATIONS

BSA	Bovine serum albumin
Ci	Curies
CMF	Cyclophosphamide, Methotrexate and 5-Fluorouacil
DNA	Deoxyribonucleic acid
Dpm	Deteriorations per minute
DTTP	Deoxythymidine triphosphate
ECM	Extracellular matrix
EDTA	Ethylenediaminetetraacetic acid
ELISA	Enzyme linked immunosorbent assay
FCS	Foetal calf serum

limited to treatment of cancer. For example, cytotoxic agents may be used for treatment of other conditions; methotrexate is widely used for treatment of severe rheumatoid arthritis.

Example 1 **Validation of human breast cancer tumours in nude mice and identification of hyaluronan receptors on the breast tumours *in situ***

To establish an appropriate animal model for human breast cancer, it was necessary to perform pathological testing. For a tumour to be physiologically viable neovascularization is essential, because the capillary network supplies nutrients to the tumour. The presence of vascularisation, ductal invasion, necrosis, apoptosis, a high mitotic index and nuclear abnormalities are all characteristic of breast carcinoma.

The human breast carcinoma cell line MDA-MB-468 (American Tissue Culture Collection, Rockville, U.S.A) was selected on the basis of its expression of the HA receptors, CD44, RHAMM and ICAM-1. Cells were routinely grown and subcultured as a monolayer in 175cm^2 culture flasks in Leibovitz L-15 Medium supplemented with 10% foetal calf serum (FCS) and 10µg/ml gentamicin. For injection into mice cells were grown to 100% confluency, trypsinised in 0.05% trypsin/0.01% EDTA solution, washed twice by centrifugation in a Beckman TJ-6 bench centrifuge (Beckman, Australia) at 400*g*av for 10min, counted using a Model-ZM Coulter counter (Coulter Electronics, England), and resuspended in serum-free Leibovitz L-15 medium at 1 x 10^8 cell/ml.

85 athymic Balb/c/WEHI nude female mice (Walter and Eliza Hall Institute of Medical Research, Melbourne, Australia), 6 to 8 weeks old, were maintained under specific pathogen-free conditions, with sterilised food and water available *ad libitum*. Ten million MDA-MB 468 cells were prepared as described above, and directly injected into the fat pad under the nipple of each mouse. Tumour

secondary antiserum (Dako, Denmark) was applied for 60min at RT, followed by 3x5min wash in PBS. Sigma *Fast* DAB (3,3'-Diaminobenzidine, Sigma, St. Louis, U.S.A) tablets were prepared according to the manufacturer's instructions and the DAB solution was applied for 5-10min at RT. The slides were washed in tap water for 10min, counterstained with haematoxylin, dehydrated and mounted.

Examination of the haematoxylin and eosin-stained breast tumour sections demonstrated all of the usual features associated with viable tumours, as shown in Figures 3 and 4, confirming that the animal host successfully maintained a grade II human breast carcinoma. There are several features which are characteristic of malignancy. The section of the slides labelled (B) displays these features. All of the pathological features of malignancy observed are in section (B), ie

i) high nuclear/cytoplasmic ratios

ii) angular chromatin and nucleoli

iii) irregular nuclear membrane

It was concluded that a grade II-III level tumour was capable of being supported in the nude mouse model. A grade II-III level tumour generally gives a prognostic survival rate of about 47% (Bloom and Richardson, 1957). A grade II-III level tumour is characterised by:

i) moderate nuclear pleomorphism, hyperchromatin, and mitotic activity, features observed throughout the displayed section of tumour; and

ii) little or no duct formation.

Large areas of necrosis (N) can be correlated with the tumour spread, which suggests a more aggressive invasive course (Carter, 1990). The infiltrating edge of the tumour is indicated by ( ).

A major aim of this experiment was validation that the histological and cytological behaviour of the tumours established in these mice were comparable to those of such tumours in their natural human hosts. In achieving this aim we have also shown that the tumour cells in the

Table 1: Expression of hyaluronan receptors on human breast tumour xenografts

The rating index for the percentage of epitope expression on the tumour was quantitated as:

0%	-
1-25%	+
26-50%	++
51-75%	+++
76-100%	++++

HA receptor	Function	Distribution on tumour	% epitope expression on tumour
CD44H	Isoform which predominantly binds and internalises HA (Culty et al., 1992)	Expressed on all cells with exception of some stromal cells	++++
CD44v6	Role in cancer unknown, but is often used as a prognostic factor. The higher the expression, the lower the survival probability (Friedrichs et al., 1995)		+
CD44v3	Often over-expressed in breast carcinoma (Friedrichs et al., 1995)		-
RHAMM	Required for transformation and tumour cell invasion (Hall et al., 1995)	Groups of infiltrating tumour cells, with high expression on cells surrounding necrotic areas	+++
ICAM-1	Binds and internalises HA, putative metabolic receptor (McCourt et al., 1994)	Present on stromal cells	++
CEA	A fetal antigen expressed on malignant cells (Haskell, 1990)	Present on all tumour cells	++++

a portion of the 24.5mg/ml MTX stock solution and dissolved overnight with vortexing, to give a final concentration of 21mg/ml. To ensure sterility gentamicin was added to a concentration of 50µg/ml and incubated overnight at 4°C. Following the addition of [^{3}H]methotrexate the HA/MTX stock mixture was diluted to injection concentration with injection grade sodium chloride. Injections were individually made according to mouse body masses, to deliver 15mg/kg MTX and 12.5mg/kg HA in 50µl. With this quantity of HA injected into the body, saturation kinetics would be observed for the period of the experiment (Fraser *et al*, 1983).

To ensure that the HA had maintained its molecular weight during the preparation of the methotrexate/HA injection mixture, the injection solution was analysed on a Sephacryl S-1000 size exclusion gel (Pharmacia, Uppsala, Sweden) with column specifications of 1.6cm x 70cm, sample size 2ml, flow rate 18ml/h and 2ml fraction size. Figure 6 shows that HA retained its molecular weight during the mixing procedure.

Mice were randomly divided into 2 groups of 40 animals. Group I received MTX only, and Group 2 received MTX/HA combination therapy. Animals were individually placed in an injection box, and the injections were administered via the tail vein. Tritiated methotrexate (mean injected disintegration's per minute (dpm) ± standard error of the mean (SEM): 19,159,146 ± 1,336,819) contained within 15mg/kg MTX ± 12.5mg/kg HA was delivered in each injection. Mice were individually housed in soft, non-wettable plastic enclosures so urine could be collected. At 30min, 1h, 2h, 4h or 8h after injection mice were anaesthetised by 0.1ml intra-peritoneal injection of Nembutal (Glaxo, Australia Pty. Ltd., Melbourne, Australia), and blood was collected from the heart or great vessels using a needle and syringe. After blood collection the animals were killed by cervical dislocation.

Blood was delivered into EDTA-coated glass tubes

The amount of MTX delivered to the bloodstream henceforth will be referred to as the "injected dose".

In order to make accurate comparisons between the sample population and normalise slight variations in organ and tumour masses, the concentration of MTX in the body organs and tumour and body fluid was expressed as % of injected dose/gram of tissue.

The mean percentage of the MTX injection remaining at the injection site was 3.78% (SEM: 0.57%). To normalise such variations, the percentage of dpm found in tumour and tissues was calculated as a percentage of the dpm injected minus the dpm found remaining at the injection site. This amount is henceforth referred to as the available dpm or available methotrexate. The results are summarised in Table 2.

No statistically significant difference was noted in the plasma levels of MTX when the drug was co-injected with HA. The gross pharmacokinetics of MTX remained unaltered, with maximum MTX plasma levels reached within 0.5 to 2h following intravenous administration (MIMS, 1997).

When possible urine was collected from the non-wettable plastic enclosures with a syringe and needle. The urine was cleared by centrifugation at 14,000g_{av} for 10 min. Its radioactive content was measured after the addition of 3ml HiSafeII scintillant to samples ranging from 8-30µl. Despite the technical difficulties in accurately quantitating the volume of urine produced by each mouse we calculated the percentage of injected MTX dose in the urine by the following formula:

$$\frac{\text{time of collection (h)} \times 42\mu\text{l} \times \text{dpm}/\mu\text{l urine} \times 100}{\text{Total dpm injected}}$$

= % of injected MTX in urine.

It was not possible to collect urine from each mouse, because of variations in the micturition rate. When 3 or more urine specimens were available per time point per treatment non-parametric statistical analysis of the data at those time points was performed. At one hour after administration there was 50% (p=0.043) more MTX in the urine of mice which received MTX/HA (see Table 2).

Immediately after killing the mouse the tumour, liver, heart, spleen, bladder, left and right kidneys, uterus, lungs, stomach, intestines, brain and lymph nodes were excised and analysed for total radioactivity. The total radioactivity in each tissue was determined by solubilising 100-400mg of tissue in 3-6ml of OptiSolv (ACC, Melbourne, Australia) for 36 h, 22°C. On completion of solubilisation, radioactivity in the tissue was counted after adding 10ml of HiSafeIII scintillant. Again to overcome chemi- and photoluminescence, samples were counted

OptiSolv for 24h at 22°C, followed by the addition of 10ml Hisafe-3 scintillant. To overcome chemi- and photoluminescence, samples were counted for 2min in a Wallac 1410 ß-counter over a 3, 7 or 20 d period depending on the sample source. During the periods between counting, samples were stored in the dark at ambient temperature. All calculations were performed on stabilised samples where all chemi- and photoluminescence had been removed.

The figures represent median ± SEM (n=8). Analysing the data with the non-parametric randomization test for matched pairs demonstrated that the co-administration of HA significantly reduced the excretion of drug into the GI tract (p=0.031, one-tailed test).

The decrease in MTX concentration ranged from 43-67%. The non-parametric randomization test for matched pairs showed that the co-administration of HA significantly reduced the excretion of drug into the gastrointestinal tract (p=0.031, one-tailed test).

In the lungs there was significantly less MTX present at 4h when co-administered with HA, with a median decrease of 52% (p=0.014). No differences were demonstrated at other time points, however, so that the significance of this observation remains uncertain.

No observable trends were detected in the spleen, uterus, brain, heart, lymph nodes, stomach and kidneys.

There are two possible mechanisms of HA targeting of methotrexate to tumour cells (Figure 10).

There was a significant targeting effect when HA was combined with MTX (Figure 7). The greatest relative increase in tumour retention of drug was observed at 0.5h (mean 24% increase), 1h (mean 30% increase) and 2h (mean 119% increase), whereas at 4h and 8h the increase was negligible. Because of the small population size and non-parametric distribution of the data the Mann-Whitney Rank Sum Test test was used, and revealed a significant increase in tumour uptake of drug when HA was co-injected. At 1h the statistical significance was p=0.021 and at 2h,

was found in the liver when it was co-injected with HA (4h: 68% less MTX and 8h: 75% less MTX). After intravenous administration MTX is widely distributed in body water, and can be retained in the liver for months (McEvoy, 1988); therefore the decreased median concentration of MTX in the liver at 4 and 8h when co-injected with HA could indicate an altered balance in the routes of pharmacokinetic clearance. Considering that HA is rapidly metabolised within the liver endothelial cells (LEC) it follows that MTX which is co-internalised with HA would be released within the liver sinusoidal lining cells, where it could either diffuse into hepatocytes to be secreted in the bile and subsequently the gastrointestinal tract, or be returned to the circulation for further distribution into body water and for urinary excretion, or both.

There could be a therapeutic advantage of short-term hepatic-targeting. In the case of liver metastasis a rapid, high exposure to MTX could be beneficial, and since the observed targeting is only for 1h this would counteract any long term toxicity problems. Liver targeting could be utilised with drugs which require bio-activation, eg mitomycin C, doxorubicin, where the drug/HA mixture would be targeted to the LEC. With the inactive drug concentrated in the LEC it would be able to diffuse into the hepatocytes for activation, thus acting as an activation targeting mechanism.

One of the major sites of toxicity of MTX is the gastrointestinal tract. Co-administration of MTX with HA significantly diminished the amount of drug delivered to the GI tract. There may be several mechanisms associated with the decreased concentration of MTX in the gut.

Methotrexate is a very small molecule, which one would expect normally to pass through most capillary walls, whereas association with HA would greatly reduce its passage through this route.

Rapid degradation of HA in the liver endothelial cells resulted in a rapid release of MTX into the liver and

as well as potentially reducing the undesired side-effect of gastrointestinal toxicity.

Example 3 **Preparation and injection of paclitaxel/ hyaluronan drug combinations**

Having established the usefulness of the nude mouse model for HA/Paclitaxel, it could now be used to test the effectiveness of other chemotherapeutics. It was decided that, due to its therapeutic importance, paclitaxel (also known as taxol) would be used.

Paclitaxel is isolated from the Western Yew, *Taxus brevifolia*, (Wani *et al* 1971), and is clinically active against advanced ovarian and breast cancer [Rownisky *et al* 1990; McGuire *et al* 1989] and is currently undergoing clinical trials for treatment of a variety of other cancers. However the main problem associated with paclitaxel is its extreme lipophilicity and consequent poor aqueous solubility. Efforts to solve this problem have led to the synthesis of paclitaxel analogues and prodrugs along with extensive efforts to devise safe and biocompatible formulations. To date no prodrugs have shown sufficient stability, solubility or activity that would warrant clinical development (Mathew *et al* 1992; Vyas *et al* 1993). However, semisynthetic taxanes are showing greater solubility and potency than paclitaxel (Bissery *et al* 1991) and one form Taxotere has entered human trials (Bisset *et al* 1993).

The current clinical formulation of paclitaxel employed for intravenous delivery utilises ethanol and Cremophor EL in a 1:1 (v/v) ratio with the drug at 6 mg/mL. Cremophor EL is actually polyethoxylated castor oil; a clear, oily viscous, yellow surfactant. Stability studies have shown that the original formulation has a shelf-life of 5 years at 4°C. The preparation is diluted before use with 0.9% saline or 5% dextrose to concentrations of 0.3-1.2 mg/mL and the physical and chemical stability of the material in these conditions is ca. 27 h. However,

50µl. With this quantity of HA injected into the body, saturation kinetics would be observed for the period of the experiment (Fraser *et al*, 1983).

To ensure that the HA had maintained its molecular weight during the preparation of the paclitaxel/HA injection mixture, the injection solution is analysed on a Sephacryl S-1000 size exclusion gel (Pharmacia, Uppsala, Sweden) with column specifications of 1.6cm x 70cm, sample size 2ml, flow rate 18ml/h and 2ml fraction size. Figure 4 shows that HA retained its molecular weight during the mixing procedure.

Mice are randomly divided into 2 groups of 40 animals. Group I received paclitaxel only, and Group 2 receive paclitaxel/HA combination therapy. Animals are individually placed in an injection box, and the injections are administered via the tail vein. Tritiated paclitaxel (mean injected disintigrations per minute (dpm) ± standard error of the mean (SEM): 19,159,146 ± 1,336,819) is delivered in each injection. Mice are individually housed in soft, non-wettable plastic enclosures so urine can be collected. At 30min, 1h, 2h, 4h or 8h after injection mice are anaesthetised by 0.1ml intra-peritoneal injection of Nembutal (Glaxo, Australia Pty. Ltd., Melbourne, Australia), and blood is collected from the heart or great vessels using a needle and syringe. After blood collection the animals are killed by cervical dislocation.

Blood is delivered into EDTA-coated glass tubes and plasma is prepared by centrifugation at 14,000g_{av} for 10 min. Radioactivity is counted in 50µl aliquots after decolourisation with 100µl of 30%v/v hydrogen peroxide and the addition of 3ml HiSafeII scintillant. To overcome chemi- and photoluminescence, samples are counted for 2min in a Wallac 1410 ß-counter over a 3, 7 or 20 d period, depending on the sample source. During the periods between counting, samples are stored in the dark at ambient temperature. All calculations are performed on stabilised samples from which all chemi- and photoluminescence had

The mean percentage of the paclitaxel injection remaining at the injection site is calculated. To normalise such variations, the percentage of dpm found in tumour and tissues is calculated as a percentage of the dpm injected minus the dpm found remaining at the injection site. This amount is referred to as the available dpm or available paclitaxel.

When possible urine is collected from the non-wettable plastic enclosures with a syringe and needle. The urine is cleared by centrifugation at $14,000g_{av}$ for 10 min. Its radioactive content is measured after the addition of 3ml HiSafeII scintillant to samples ranging from 8-30µl.

Immediately after killing the mouse the tumour, liver, heart, spleen, bladder, left and right kidneys, uterus, lungs, stomach, intestines, brain and lymph nodes are excised and analysed for total radioactivity. The total radioactivity in each tissue is determined by solubilising 100-400mg of tissue in 3-6ml of OptiSolv (ACC, Melbourne, Australia) for 36 h, 22°C. On completion of solubilisation, radiactivity in the tissue is counted after adding 10ml of HiSafeIII scintillant. Again to overcome chemi- and photoluminescence, samples are counted for 2min in a Wallac 1410 ß-counter over a 3, 7 or 20 d period depending on the sample source. During the periods between counting, samples are stored in the dark at ambient temperature. All calculations are performed on stabilised samples from which all chemi- and photoluminescence had been removed.

Example 4 Use of 5-Fluorouracil and HA

Introduction

5-Fluorouracil is (5-FU) an antimetabolite that is commonly used in the treatment of breast and gastrointestinal tract cancers (Piper & Fox, 1982). 5-FU is converted to its active nucleotide form intracellularly where it interferes with both DNA and RNA synthesis. The drug functions via two mechanisms *in vivo*:

Example 5 Investigation of the synergistic action of 5-FU and HA in human breast cancer cells

Human breast adenocarcinoma cell lines MDA-MB-468, MDA-MB-435 and MDA-MB-231 were selected based on HA binding affinity (Culty *et al*, 1994) and the expression of the HA receptors of CD44 and RHAMM (Wang *et al*, 1996). Summaries of the cell line characteristics are shown in Table 3.

Cell lines MDA-MB-468, MDA-MB-435 and MDA-MB-231 were routinely cultured as described in example 1.

It can be seen from Table 4 that breast cancer cells grown in media containing 0nM 5-FU + 100nm of HA did not demonstrate a statistically significant proliferative or cytotoxic effect when compared to untreated cells.

Therefore all results were expressed as a percentage of the 0nM 5-FU/0nM HA cell count. Distinct differences in growth patterns were noted between cell lines, for example MDA-MB-231 and MDA-MB-468 cells demonstrated a poor plating efficiency, where numerous floating cells were present before application of the test media. The MDA-MB-435 cell line demonstrated a high plating efficiency and a very rapid growth rate.

When HA was combined with 5-FU a syngeristic cytotoxic effect was observed with the MDA-MB-468 cell line, but not with the MDA-MB-231 or MDA-MB-435 breast cancer cell lines. This is shown in Figure 11. The IC_{50} of 5-FU alone was >50μm, but when combined with HA the IC_{50} was 40nM, a reduction in drug dosage of up to 1250 times.

The results from the *in vitro* experiments demonstrated an increase in cell kill when 5-FU was applied to the breast cancer cells in the presence of HA. The MDA-MB-468 cells showed the greatest susceptibility to the 5-FU/HA therapy where the IC_{50} was decreased from >50μM to 40nM, whereas both the MDA-MB-231 and MDA-MB-435 were not greatly affected by the 5-FU/HA combination. All of the breast cancer cell lines expressed high levels of the CD44 receptor with the MDA-MB-468 (60-80%), MDA-MB-231 (40-60%) and MDA-MB-435 (40-60%) as determined by Culty *et al* (1994). It has been demonstrated that the three cell lines used in these experiments are able to degrade HA, implying that the function of CD44 in tumour cells may be to mediate the degradation of HA (Culty *et al*, 1994).

Another factor to consider is the previous exposure of the cells to chemotherapeutic drugs. Before a cancer cell line is isolated from a patient, the cancer sufferer has often undergone chemotherapy or radiation, which could result in the tumour containing treatment-resistant cells. In the case of MDA-MB-435 and MDA-MB-231 the patients from which the cell lines were derived had both been previously exposed to 5-FU (Cailleau *et al*, 1974). Since cancer cells contain several adaptation

specifications of 1.6cm x 70cm, sample size 2ml, flow rate 18ml/h and 2ml fraction size. The HA was used at a final concentration of 100nM, with all dilutions made in the appropriate growth medium.

The stock solution of 5-FU was prepared by dissolving 5-FU in 0.1M sodium hydroxide and brought to a concentration of 20mg/ml with 0.9%w/v pyrogen-free injection grade NaCl. The stock solution was filtered through a 0.22µm filter to ensure sterility before addition of [^{3}H]-FU and dilution to injection concentration with injection grade sodium chloride. Individual injections were prepared according to individual mouse masses, with the aim of delivering 30mg/kg 5-FU in 50µl (equivalent to human therapeutic dose of 10.5mg/kg for a mean body weight of 60kg; Inaba *et al*, 1988). A pyrogen-free, HA stock solution (10mg/ml; modal M_r $7x10^5$ Da) was added to a portion of the 20mg/ml 5-FU stock solution and incubated overnight with vortexing, to a final HA concentration equivalent to 12.5mg/kg of mouse mass. Injections were individually made according to mouse masses, to deliver 30mg/kg 5-FU and 12.5mg/kg HA in 50µl. With this quantity of HA injected into the body, saturation kinetics would be observed for the period of the experimentation (Fraser *et al*, 1983). To ensure that the HA had maintained its molecular weight during the preparation of the injection mixture, the injection solution was analysed on a Sephacryl S-1000 size exclusion gel with column specifications of 1.6cm x 70cm, sample size 2ml, flow rate 18ml/h and 2ml fraction size. Hyaluronan was detected in column fractions by the uronic acid assay.

The uronic acid assay was used to detect the presence of hyaluronan qualitatively from the fractions collected from the gel filtration chromatography procedure. A 25µl aliquot of each fraction was then transferred into a 96 well plate. 250µl of a carbazole reagent (3M carbazole/0.025M borate in H_2SO_4) was then added to these fractions. The 96 well plate was incubated for 45-60min at

and cells were counted with a Coulter Counter.

Example 8 Evaluation of HA as a drug delivery and tumour-targeting vehicle

Based on the results from the drug sensitivity *in vitro* experiments as described in examples 5 to 7, and the expression of the HA receptors of CD44 and RHAMM, the human breast carcinoma cell line MDA-MB-468 was selected as the cancer cell inoculant for the generation of any nude mouse human tumour xenografts. Cells were routinely grown and subcultured as a previously described in example 5. For injection into mice, cells were grown to 100% confluency, trypsinised in 0.025% trypsin/0.01% EDTA solution, washed twice by centrifugation in a Beckman TJ-6 bench centrifuge at $400g_{av}$ for 10min, counted using a Model-ZM Coulter counter and resuspended in serum-free Leibovitz L-15 medium at 1×10^8 cells/ml.

The athymic CBA/WEHI nude female mice, 6 to 8 weeks old, were maintained under specific pathogen-free conditions, with sterilised food and water available ad libitum. Each mouse received one injection containing 5×10^6 cells in 50µl. The cells were injected with a 26 gauge needle into the mammary fat pad directly under the first nipple (Lamszus *et al*, 1997). Tumour measurements were made weekly by measuring three perpendicular diameters ($d_1d_2d_3$). Tumour volume was estimated using the formula:

$$(1/6)\pi\ (d_1d_2d_3)$$

Treatment with 5-FU ± HA was commenced approximately 4-8 weeks after the cancer cell inoculation. The mean tumour size for mice used in each study is summarised in Table 5.

To establish the tumorigenicity of breast cancer cell line MDA-MB-468 and its ability to generate tumours upon injection into an appropriate animal host, it was necessary to perform pathological testing. For a tumour to be physiologically viable neovascularisation is essential where the capillary network supplies nutrients to the tumour. The presence of vascularisation, ductal invasion, necrosis, apoptosis, a high mitotic index and nuclear abnormalities are all characteristic of breast carcinoma. Examination of the haematoxylin and eosin stained breast tumour sections demonstrated all of these features, so confirming that the animal host successfully maintained a grade II human breast carcinoma.

Approximately 8 weeks after tumour induction two tumour-bearing mice were given a lethal dose of Nembutal. Within 3min of killing the mice, tumours were surgically removed and immediately fixed in 10% buffered formalin for 12h. The fixed tumour was dehydrated overnight in a series of 70-100% ethanol, followed by paraffin embedding from which 2-4 µm sections were cut. The sections were placed on slides, de-waxed, and brought to water. Slides were washed 3x5min in PBS. Heterophile proteins were blocked by incubation with 10% foetal calf serum for 10min, followed by a PBS rinse. The detection antibodies were applied for 60min at RT. The detection antisera or antibodies were against RHAMM, CD44H and CAE. The slides were washed 3x5min in PBS and endogenous peroxidase activity blocked by immersion in 0.3%H_2O_2 in methanol for 20min. Following a further PBS wash, the peroxidase-conjugated pig anti-rabbit secondary antiserum was applied for 60min at RT, followed by 3x5min washes in PBS. Sigma Fast 3,3'-Diaminobenzidine tablets (DAB) were prepared according to the manufacturer's instructions and the DAB solution was applied for 5-10min at RT. The slides were washed in tap water for 10min, counterstained with haematoxylin, dehydrated and mounted.

The human origin of the tumour was confirmed by staining the tumour and surrounding tissue with a human-

Table 6: Distribution of HA receptors on human breast cancer tumours grown in nude mice

HA receptor	Function	Distribution on tumour	% epitope expression on tumour
CD44H	Isoforms which bind and internalise HA (Culty *et al*, 1992)	Expressed on all cells except for a few stromal cells	+ + + +
CD44 v 6	Functional role in cancer unknown however the higher the expression results in a diminished survival probability (Friedrichs *et al*, 1995)	Some infiltrating tumour cells	+
CD44 v 3	Over-expression often found in breast carcinoma (Friedrichs *et al*, 1995)		-
RHAMM	Necessary for transformation and tumour cell invasion (Hall *et al*, 1995)	Groups of infiltrating tumour cells, with high expression on cells surrounding necrotic areas.	+ + +
CEA	A foetal antigen expressed on malignant cells (Haskell, 1990)	Expressed on all tumour cells	+ + + +

Rating index for percentage of epitope expression on tumour:

0 % : -
1-25 %: +
26-50 % : + +
51-75 % : + + +
76-100 % : + + + +

10min. Radioactivity was counted in 50µl after decolourisation with 100µl of hydrogen peroxide, 30%v/v and the addition of 3ml HiSafeII scintillant. To overcome chemi- and photoluminescence, samples were counted for 2min in a Wallac 1410 ß-counter over a 3, 7 or 20 d period depending on the sample source. During the periods between counting, samples were stored in the dark at ambient temperature. All calculations were performed on stabilised samples where all chemi- and photoluminescence had disappeared. To determine the percentage of injected 5-FU in the plasma, it was necessary to calculate the total plasma volume of each mouse (ml). The standard formula was:

Mouse Mass (g) X mouse blood volume (0.07) X plasma proportion of blood (0.59)[1]

The percentage of injected 5-FU in the plasma was calculated by:

$$\frac{\text{Plasma volume (ml) X dpm/ml plasma X 100}}{\text{total dpm injected}}$$

When possible urine was collected from the non-wettable plastic enclosures with a syringe and needle. The urine was cleared by centrifugation at 14,000gav for 10min. Its radioactive content was measured after the addition of 3ml HiSafeII scintillant to samples ranging from 8-30ul. Through the technical difficulties in accurately quantitating the volume of urine produced by each mouse the % of the injected 5-FU dose in the urine was calculated by the following formula:

$$\frac{\text{time of collection (h) x 42µl}^{1}\text{ x dpm/ul urine x 100}}{\text{total dpm injected}}$$

Once blood was taken, the mice were killed by

Table 7: Effect of hyaluronan on the biodistribution of [^{3}H]5-Fluorouracil in nude mice bearing human breast carcinoma xenografts

	5-FU (mean % dose/g ± 1 SE, n=5)					HA/5-FU (mean % dose/g ± 1 SE, n=5)				
	10 min	**20 min**	**30 min**	**1 h**	**2 h**	**10 min**	**20 min**	**30 min**	**1 h**	**2 h**
Tumour	1.49±0.25	2.13±0.28	1.20±0.17	1.34±0.1	1.35±0.24	3.60±0.35	3.20±0.22	2.45±0.14	1.85±0.23	1.03±0.12
Liver	19.64±3.75	23.27±1.6	15.86±3.12	9.20±1.83	3.64±1.09	21.2±1.81	21.37±1.71	15.98±1.68	8.73±1.92	3.99±1.24
Spleen	1.45±0.28	1.71±0.18	1.02±0.13	1.02±0.07	0.99±0.09	1.94±0.17	1.39±0.12	1.17±0.20	1.3±0.19	1.21±0.18
Lymph Nodes	2.04±0.31	2.98±0.78	1.49±0.27	1.72±0.46	0.88±0.17	3.47±0.61	2.99±0.47	1.97±0.22	1.85±0.29	0.75±0.12
Kidneys	5.15±1.42	12.53±2.37	10.12±2.01	7.39±1.12	3.97±0.71	9.24±0.91	14.56±0.94	14.52±1.56	10.72±1.97	5.51±0.98
Bladder	18.30±3.98	40.34±26.39	19.11±10.76	33.69±18.72	61.88±39.1	13.31±5.18	39.17±20.74	37.95±25.1	10.04±5.53	6.05±3.58
Intestines	1.33±0.24	1.73±0.42	2.39±0.76	1.57±0.23	2.44±1.42	1.64±0.28	2.06±0.25	1.90±0.08	1.30±.23	1.79±0.62
Stomach	1.59±0.35	1.25±0.40	1.11±0.26	1.58±0.33	0.76±0.18	2.44±0.52	2.98±0.38	1.63±0.19	1.58±0.11	1.48±0.62
Brain	0.34±0.02	0.50±0.07	0.37±0.06	0.48+0.04	0.55+0.04	0.60±0.06	0.66+0.03	0.59±0.06	0.58+0.04	0.58+0.03
Heart	1.26±0.21	1.51±0.19	1.01±0.11	***0.81±0.05***	***0.68±0.08***	1.67±0.28	1.56±0.11	1.03±0.19	***0.48±0.10***	***0.36±0.05***
Lungs	1.61±0.35	2.48±0.45	1.46±0.20	1.15±0.10	0.84±0.01	2.21±0.27	2.23±0.21	2.13±0.19	1.45±0.06	0.92±0.07
Bone	1.37±0.30	1.36±0.13	0.86±0.14	0.89±0.06	0.86±0.18	2.01±0.07	1.78±0.13	1.18±0.09	1.08±0.19	0.66±0.05
Uterus	1.88±0.42	2.52±0.22	1.63±0.24	1.51±0.24	1.57±0.60	3.38±0.35	3.41±0.47	2.17±0.21	1.78±0.28	1.36±0.45
Plasma	***6.26±0.57***	***5.32±0.80***	2.59±0.20	***1.88±0.13***	1.36±0.3	***2.76±0.18***	***2.76±0.36***	2.50±0.28	***1.01±0.05***	0.85±0.09

12 point bold represents measurements where the co-administration of HA significantly reduced the 5-FU concentration (Students t-test)

represents measurements where the co-administration of HA significantly increased the 5-FU concentration (Students t-test)

Example 10 Administration of treatment regimens to mice

One of the most commonly used treatment regimens for human breast cancer is cyclophosphamide, methotrexate and 5-fluorouacil which is administered on day 1 and 8 of a 28 day cycle. In human breast cancer the initial treatment regimen is for 6 cycles at which time the patient condition is re-assessed, therefore we tried to simulate the human treatment regimen as closely as possible by exposing the mice to 6 cycles (6 months) of treatment in a long term efficacy study and a 6 cycles (6 week) short term efficacy study. Considering the life cycle of a mouse is approximately 2 years we commenced both short-term and long-term treatment protocols as shown in Table 8.

Mice were randomly divided into 7 groups of 8 animals per group for the short term study and 5 groups of 8 animals for the long term study (refer to Table 8 for dosage and treatment administration schedule).

The treatment was not extended over the 6 month regimen since it has been demonstrated that chemotherapy lasting more than six months has not generally been associated with greater benefit (Harris *et al*, 1992).

Animals were weighed and tumour volumes measured on the day of treatment application for long term study as described in Example 8. In the 6-week study animals were weighed and tumour volumes measured on a daily basis. Animals were individually placed in an injection box, and the injections were administered via the tail vein. It has been experimentally proven that stress can be a major factor in a patients response to chemotherapy (Shackney et al, 1978), therefore we ensured that equal numbers of mice were allocated to each cage, the animal number per cage varied from 5-8 depending on the stage of experimentation.

The experimental end-point occurred when the animal had to be euthanised due to degree of disease progression or when the 6 month (long term) or 6 week (short term) treatment regimen was completed. Due to the animal ethics guidelines the animals were monitored fortnightly by an independent animal ethics officer who assessed the degree of disease progression. As shown in Figure 16, the following criteria were used to determine if an animal had reached the stage of experimental end-point of necessary death:

1). animal was not eating or drinking and had experienced dramatic weight loss;

2). tumour size was greater than 10% of body mass (Panel A);

3). tumour mass was so large the animal was immobilised (Panel B).

At the experimental end-point the animals were anaesthetised by a 0.1ml intra-peritoneal injection of

were examined by Dr P. Allen (certified pathologist) where each node was microscopically examined for the presence of tumour cells. The CEA immunostained lymph nodes were microscopically examined, where any positively stained nodes were counted and considered positive for lymph node metastasis.

Tumour volume was monitored on a daily or weekly basis by calliper measurements and tumour volume calculated as previously described in example 8.

One of the most common toxic effects of 5-FU is on the gastro-intestinal tract where haemorrhagic enteritis and intestinal perforation can occur (Martindale, 1993). Animals were monitored daily for GI tract upset such as diarrhoea and weekly for more severe toxicity manifestations such as weight loss. Weight loss was monitored by calculating net body weight as estimated by subtracting tumour weight, which was calculated as 1g x tumour volume (cm^3) as cited in Shibamoto *et al*, 1996. For demonstration of any weight changes the animal body weight was normalised to the body weight at the time of treatment commencement as:

$$\frac{\text{Body mass (ex tumour)} - \text{body mass at commencement of treatment (ex tumour)}}{\text{Body mass at commencement of treatment (ex tumour)}} \times 100$$

No daily GI tract upset such as diarrhoea was noted in any of the animals regardless of treatment regimen. Severe gastro-intestinal toxicity for each treatment regimen was estimated using loss of body weight (excluding the tumour weight) as an indicator. At the time of death of each animal the percentage change in body mass was calculated as previously described. There was a statistically significant difference in the normalised body weight between the saline, HA, 5-FU treatment groups as compared to the 5-FU/HA group treatment group (Figure 18). The mice receiving the 5-FU/HA adjuvant therapy demonstrated a 16% increase in body weight (students t-test, p=0.025) throughout the treatment in comparison to

Table 9A The Effect of 5-FU/HA Adjuvant Therapy on the Growth and Metastasis of Human Breast Cancer Xenografts in Nude Mice: 6-Week Study

Treatment Group	TDT Mean± SEM	% of animals with lymph node metastasis	Number of new tumours	% of lymph node involved per animal mean ± SEM	Number of animal completing treatment	% change in body weight mean ± SEM
1. Saline	9.4 ± 1.1	100	3	94.2 ± 2.8	8/8	100.1 ± 0.61
2. 5-FU/HA	20.9 ± 2.7	100	0	12.1 ± 0.9	8/8	116.0 ± 0.56
3. HA D1,2	27.7 ± 5.2	100	0	18 ± 4.1	8/8	102.5 ± 0.38
4. 5-FU D1,2	32.1 ± 3.5	100	1	14.3 ± 2.9	8/8	97.5 ± 0.73
5. HA followed by 5-FU	14.8 ± 3.7	To be assessed	To be assessed	To be assessed	8/8	101.8 ± 0.93
6. HA D1,3	30.7 ± 4.9	To be assessed	To be assessed	To be assessed	8/8	100.9 ± 0.56
7. 5-FU D 2, 4	15.3 ± 2.5	To be assessed	To be assessed	To be assessed	8/8	98.3 ± 0.73

Example 11 Long-term treatment: 6-month regimen

While this study is still on-going there are significant data being generated.

The TDT is the time taken (days) for a tumour to double in mass or cell number, a parameter of tumour growth which is simple to measure and can be easily related to clinical tumour behaviour in conceptional terms (Shackney *et al*, 1978). By monitoring the tumour doubling time it is often possible to evaluate tumour chemotherapeutic response, as slowly growing tumours tend to respond poorly to chemotherapy (Schabel, 1975).

The tumour doubling time for each treatment is shown in Table 9B.

There was not a significant difference in TDT between the 5-FU/HA and 5-FU treatment. As with the 6-week study, the administration of HA also demonstrated a therapeutic effect on the primary tumour, demonstrating a TDT of 26±1.75 versus the saline of 13±4 days. The administration of HA 24h before 5-FU appeared to counteract any therapeutic value of 5-FU in relation to retardation of tumour growth.

Tumour mass and volume are useful parameters in monitoring tumour treatment response and progression, but do not ultimately demonstrate the cytotoxic effects rendered by a therapy. We wanted to establish if the HA/5-FU therapy killed more tumour cells and the location of the cells. Dying cells can be pathologically manifested by:

i). disintegration of the nucleus (apoptosis)

ii). lysis of the cell (necrosis)

Scanning the entire tumour image into an MCID computer that calculated the entire tumour area quantitated the number of dying cells. The cells with fragmented nuclei or lysed cells were outlined and scanned, these areas which are then digitised and the exact area of dying cells calculated. The percentage of the tumour attributed to dead cells was calculated by:

$$\frac{\text{area of apoptotic and necrotic cells X 100}}{\text{area of entire breast tumour}}$$

A viable cell contains more water than a dying or dead cell, therefore by determining the ratio of dry tumour mass to wet tumour mass it is possible to estimate the overall area of viable versus non-viable cells. The tumours were dissected bilaterally where half was processed for tumour pathology and the remaining half was weighed before and after drying at 50°C for 48h. The dry mass as a percentage of wet tumour mass was calculated by:

$$\frac{\text{Dry tumour mass X 100}}{\text{Mass of wet breast tumour}}$$

and HA groups, as shown in Figure 21.

Conclusions

The data from the 5-FU targeting show that there was a statistically significant increase in 5-FU uptake by tumours when 5-FU was injection with HA at the time points 10, 20 and 30 minutes with a 2.4, 1.5 and 2 fold increase respectively in 5-FU uptake (Table 7). This indicated that 5-FU was being targeted to the tumour by the HA. There are two possible mechanisms of HA targeting of 5-FU to tumour cells:

HA containing associated 5-FU binds to the receptors (CD44) and is internalised via receptor-mediated endocytosis, so releasing the drug into the tumour cell.

The HA molecular mesh will act as an impedance to outward diffusion, so that after HA binds to receptors (CD 44 and RHAMM), the entrained 5-FU is able to diffuse into the tumour cells. While held at the surface of the cells by the HA matrix the 5-FU has increased availability to the active transport mechanism normally utilised for 5-FU transport into the underlying cell.

The catabolism of HA mainly occurs in the lymph nodes (Fraser *et al*, 1988) and the liver (Laurent *et al*, 1986). HA is normally cleared from the blood stream by receptor-mediated cellular uptake and catabolism in the liver (80-90%), kidneys (10%), spleen (0.1%) and bone marrow (0.1%)." (Fraser *et al*, 1983). Circulating HA is taken up by the metabolic receptor, also known as the liver endothelial cell (LEC) receptor (Eriksson *et al*, 1983), whereas the CD44 receptor appears to be involved with HA internalisation associated with cellular processes instead of metabolism, while the RHAMM receptor is only involved in cell motility. Combining HA with 5-FU could result in high levels of 5-FU being targeted to the sites of HA or 5-FU metabolism. The data from the targeting experiments (Table 6) shows that there was no significant increase in 5-FU targeting to the liver when administered with HA. As no

(Underhill *et al* 1993), which could account for the increased targeting. This could be associated with a therapeutic advantage in the treatment of carcinoma of the lung, where small and large cell lung carcinomas have been reported to contain an over expression of CD44 and RHAMM (Horst *et al*, 1990).

The was a significant decrease in 5-FU targeted to the heart at the 1 and 2 h time points when HA was co-injected with 5-FU. As 5-FU administration can result in cardiotoxicity (MIMS, 1997) administration of 5-FU with HA may reduce the degree of toxicity to the heart compared to when 5-FU is administered alone.

When evaluating the therapeutic efficacy of the HA/5-FU adjuvant therapy several observations were consistent throughout both the long and short-term treatment protocols.

Mice receiving HA/5-FU or HA alone appeared to have more energy and maintain or increase body mass, observations supported by the increased survival times of HA/5-FU mice in the 6-month study

Tumours of mice receiving 5-FU/HA or HA developed areas of external necrosis, to the extent where 2 tumours dropped off

The addition of HA to 5-FU did not appear to have a significant effect on the volume of the primary treatment when the therapy was administered for 6 weeks, but this could be due to the vasculature of the tumour. Tumours consist of three areas. When HA was administered with and without 5-FU it would reach the tumour, enter the well vascularised and semi-necrotic areas via the large gap junctions of the damaged blood vessels. Due to the ability of HA to absorb water this could result in an influx in extracellular fluid to the necrotic area of the tumour, subsequently increasing the volume of the tumour and causing further damage to tumour vasculature. This hypothesis is consistent with the observation that tumours treated with HA±5-FU did routinely demonstrate necrosis and

Table 10 Common Results and Differences Between Adjuvant Therapy with MTX/HA and 5-FU/HA

5

Study	Similar Results	Different Results
MTX/HA: 6-month VS 5-FU/HA: 6-week	Mice receiving HA/drug experienced significant weight gain; No marked increase in patient survival; Inhibited formation of new tumours; Demonstrated a longer TDT; Reduced lymph node metastasis	
MTX/HA 6-month VS 5-FU/HA 6-month	Demonstrated a longer TDT	5-FU/HA mice demonstrate increased survival
HA control for MTX/HA: 6 month VS HA control for 5-FU/HA: 6 week & 6 month		HA mice in the 5-FU/HA study demonstrated that HA exerted a therapeutic effect by reducing TDT; HA reduced lymph node metastasis and tumour formation.

References

Adams JD, Flora KP, Goldspiel BR, Wilson JW, Finley R, Arbuck SG and Finley R, 1993. *J. Natl. Cancer. Inst. Monographs* 15:23-27.

Akima, K., Ho, H., Iwata, Y., Matsuo, K., Watari, N., Yanagi, M., Hagi, H., Oshima, K., Yagita, A., Atomi, Y., and Tatekawa, I. (1996) Evaluation of antitumor activities of hyaluronate binding antitumor drugs : Synthesis, characterization and antitumor activity. *Jpn J Drug Targeting* 4: pp 1-8

Arch R, Wirth K, Hofmann M, Ponta H, Matzku S, Herrlich P and Zoller M, 1992. *Science* 257(5070):682-685.

Auvinen, P.K., Parkkinen, J.J., Agren, U.M., Johansson, R.T., Tammi, R.H., Eskelinen, M.J. & Kosma, V.M. (1997) Expression of hyaluronan in benign and malignant breast lesions. *Int. J. cancer.* 74: pp.477-481

Bartolazzi A, Peach R, Aruffo A and Stamenkovic I, 1994. *J Exp Med* 180:53-66.

Bissery M, Guenard D and Lavelle F, 1991. *Cancer Res* 51:4845-4852.

Bisset D, Setanioans A, Cassidy J, Graham MA and Kerr DJ, 1993. *Cancer Res* 53:523-527.

Bitter, T., and Muir, HM. (1971) Carbazole Assay for the quantitation of uronic acid compounds. *Anal. Biochem.* 4: pp. 330-334

Brown, M.B., Marriott, C. and Martin, G.P. (1995) A study of the transdermal drug delivery properties of hyaluronan. In: Third International Workshop on Hyaluronan in Drug Delivery. (Editor: Willoughby, D.A) Round Table Series 40. Roy.Soc.Med.Press. pp.53-73

Brown, TJ., Akon, D. and Fraser, JRE (1999) Absorption of hyaluronan applied to the surface of the skin. *J. Invest Dermatol* 103: pp 113-119

Cailleau, R. (1974) Breast cancer cell lines *J NatI Cancer Inst* 55 : pp 661-674

Carter D, 1990. *Interpretation of Breast*

Fraser, J.R.E. and Laurent, T.C. (1996) Hyaluronan. In: Extracellular Matrix. (Editor: Comper, W.D.) Harwood Academic Publishers, New York Volume 2:pp. 141-199

Fraser, JRE. and Laurent, TC. (1989) Turnover and metabolism of hyaluronan. In: The Biology of Hyaluronan. (Editors: Evered, D. and Whelan, J) Ciba Foundation Symposium 143. J Wiley and Sons, Chichester. pp.41-59

Fraser, JRE., Appelgren, LE. and Laurent, TC. (1983) Tissue uptake of circulating hyaluronic acid. A whole body autoradiographic study. *Cell Tissue Res* 233(2): pp285-293

Fraser, JRE., Kimpton, WG., Laurent, TC., Cahill, RNP. and Vakais, N. (1988) Uptake and degradation of hyaluronan in lymphatic tissue. *Biochem. J.* 256: pp. 153-158

Fraser, JRE., Laurent, TC., Pertoft, H. and Baxter, E. (1981) Plasma clearance, tissue distribution and metabolism of hyaluronic acid injected intravenously in the rabbit. *Biochem. J.* 200: pp. 415-424

Freemantle, C.N., Seed, M.P., Brown, J., Alam, C.A.S., Asculai, S. and Willoughby, D.A. (1995). The inhibition of tumour growth by topical hyaluronan and diclofenac-sodium in combination (HYAL EX-0001). In: Third International Workshop on Hyaluronan in drug delivery. (Editor: Willoughby, D.A) Roy.Soc.Med.Press. pp. 89-97

Friedrichs G, Folker HJ, Arlt PA and Gunthert U, 1995. *The Lancet* 345:1237-1238.

Gullino, PM. (1966) The internal milieu of tumors. *Progr Exp Tumor Res* 8: pp 1-25

Günthert U, 1993. *Curr Topics Microbiol Immunol* 184:47-63.

Gustafson S, Björkman T, Forsberg N, Lind T, Wikström T and Lidholt K, 1995. *Glycoconjugate J* 12:350-355.

Hall CL, Yang B, Yang X, Zhang S, Turley M, Samuel S, Lange LA, Wang C, Curpen GD, Savani RC, Greenberg

Kazuo, A., Hisashi, ITO., Yuhei, I., Kayoko, M., Nobutoshi, W., Mitsuo, Y., Hiroo, H., Kazumi, O., Akikuni, Y., Yutaka, A. and Isao, T. (1996) Evaluation of antitumor activities of hyaluronate binding antitumor drugs: synthesis, characterization and antitumor activity. *Journal of Drug Targeting*. 4:pp.1-8

Klein ES, He W, Shmizu S, Ascula S, Falk RE, 1994. *Royal Soc Med Round Table Series* 33:11-15.

Lamszus K, Jin L, Fuchs A, Shi E, Chowdhury S, Yao Y, Polverni PJ, Laterra J, Goldberg ID and Rosen EM, 1997. *Lab Inv* 76(3):339-353.

Lamszus, K., Jin, L., Fuchs, A., Shi, E., Chowdhury, S., Yao, Y., Polverni, PJ., Laterra, J., Goldberg, ID. and Rosen, EM. (1997) Scatter factor stimulates tumour growth and tumour angiogenesis in human breast cancers in the mammary fat pads of nude mice. *Lab Inv* 76(3): pp 339-353

Lapcik, L., Lapcik, Jr.L., Smedt, SD., Demeester, J. and Chabrecek, P. (1998) Hyaluronan: Preparation, Structure, and Applications. *Chemical Reviews*.Vol: 98, No 8:pp.2663-2684

Larsen, N.E. and Balazas, E.A. (1991) Drug delivery systems using hyaluronan and its derivatives. *Adv. Drug Delivery Rev.* 7:p.279

Laurent, T.C, 1970. In: *Chemistry and Molecular Biology of the Intercellular Matrix*. (Editor: Balazs, E.A.) Academic Press, New York. 2: pp. 703-732.

Laurent, T.C. (1989) In: The biology of hyaluronan. (Editors: Evered, D. and Whelan, J.) Ciba Foundation Symposium 143. J Wiley and Sons, Chichester. pp.1-5

Laurent, TC., Fraser, J.R.E., Pertoft, H. and Smedsrod, B. (1986) Binding of hyaluronate and chondroitin sulphate to liver endothelial cells. *Biochem J.* 234: pp.653-658

Lebel, L., Gabrielsson, J., Laurent, TC. and Gerdin, B. (1994). Kinetics of circulating hyaluronan in

Workshop on Hyaluronan in drug delivery. (Editor: Willoughby, D.A) Roy.Soc.Med.Press. pp.110-121

Moreira, CA., Moreira, AT., Armstrong, DK., Jellife, RW., Woodford, CC., Liggett, PE. and Trousdale, MD. (1991) In vitro and in vivo studies with sodium hyaluronate as a carrier for intraocular gentamicin. *Acta Opthalmol*. 69:pp 50-56

Nelson, JA. and Falk, RE. (1994) Anticancer research . *Int J Cancer Res Treat*

Nikaido N, 1993. *Science* 264:382-388.

Ning, S., Trisler, K., Brown, DM., Yu, NY., Kanekal, S., Lundsten, MJ. and Knox, SJ. (1996) Intratumoral radioimmunotherapy of a human colon cancer xenograft using a sustained-release gel. *Radiotherapy and Oncology*. 39: pp 179-189

Ogawa Y, Hirakawa K, Nakata B, Fujihara T, Sawada T, Kato Y, Yoshikawa K and Sowa M, 1998. *Clin Cancer Res* 4(1):31-36.

Olivotto, I. (1995) Intelligent patient guide to breast cancer

Parker, SL., Tong, T., Bolden, S. and Wingo, PA. (1996) Cancer statistics. 1996. *CA Cancer J Clin* 46:5-27.

Piper, AA. and Fox, M. (1982) Biochemical basis for the differential sensitivity of human T- and B-Lymphocyte lines to 5-fluorouracil. Cancer Research 42 : pp 3753-3760

Preston, BN., Davies, M. and Ogston, AG. (1985) The composition and physiological properties of hyaluronic acids from ox synovial fluild and from case of mesothelioma. *Biochem J* 96: pp 449-74

Ropponen, K., Tammi, M., Parkkinen, J., Eskelinen. M., Tammi, R., Lipponen, P., Agren, U., Alhava, E. & Kosma, V.M. (1998) Tumor cell-associated hyaluronan as an unfavorable pronostic factor in colorectal cancer. *Cancer Res*. 58: pp. 342-347

Rownisky EK, Cazenave LA and Donehower RC, 1990.

4(3):567-76.

Wang, C., Tammi, M., Guo, H. and Tammi, R. (1997) Hyaluronan distribution in the normal epithelium of esophagus, stomach, and colon and their cancers. *American Journal of Pathology*. 148 (6): pp 1861-1869

Wang, C., Zhang, S. and Turley, EA. (1996) The role of hyaluronan and hyaluronan receptors in breast cancer cell invasion, motility and proliferation.In: Fourth International Workshop on Hyaluronan in Drug Delivery. (Editor: Willoughby, D.A) Roy.Soc.Med.Press. pp 37-53

Wani MC, taylor HL and Wall ME, 1971. *J. Am. Chem. Soc* 93:2325-2327.

Waugh W, Trissel L and Stella VJ, 1991. *Am. J. Hosp. Pharm* 48: 1520-1524.

Weiss RB, Donehomer RC, Weirnik PH, Ohnuma T, Gralla RJ, Leyland-Jones B, 1990. *Br. J. Clin. Oncol* 8:1263-1268.

Yerushalmi, N., Arad, A. and Margalit, R. (1994) Molecular and Cellular Studies of Hyaluronic Acid-Modified Liposomes as Bioadhesive Carriers for Topical Drug Delivery in Wound Healing. *Arch of Biochemistry and Biophysics*. 113 (2) :pp 267-273

A: Possible Interactions Between Methotrexate and Hyaluronan

i: Ionic bonding

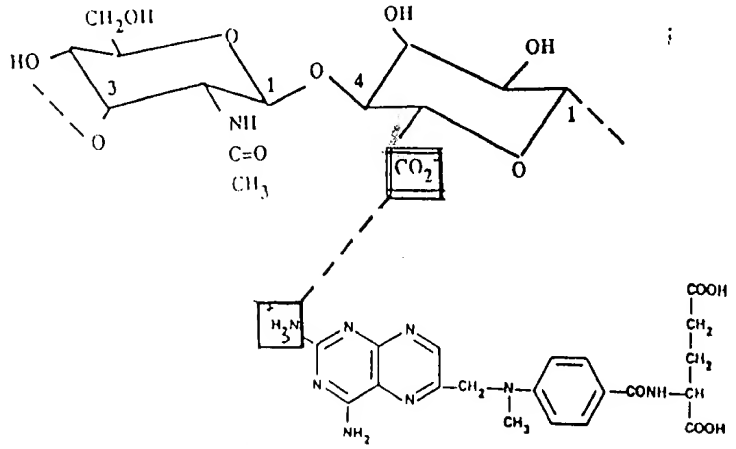

ii: Hydrogen Bonding

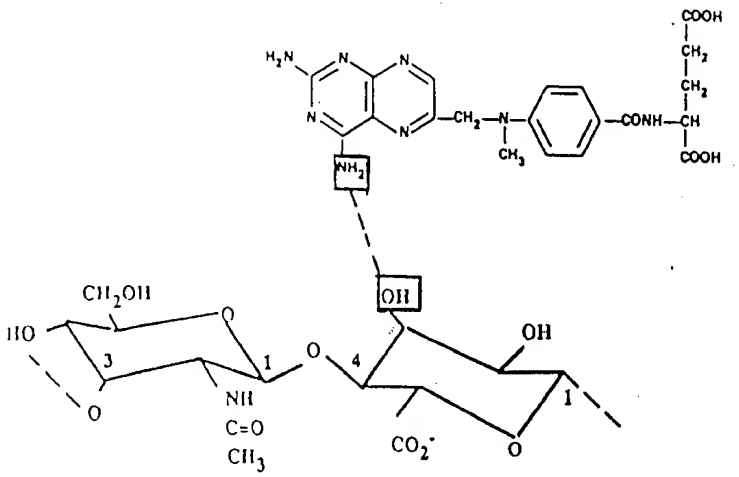

iii: Hydrophobic Bonding

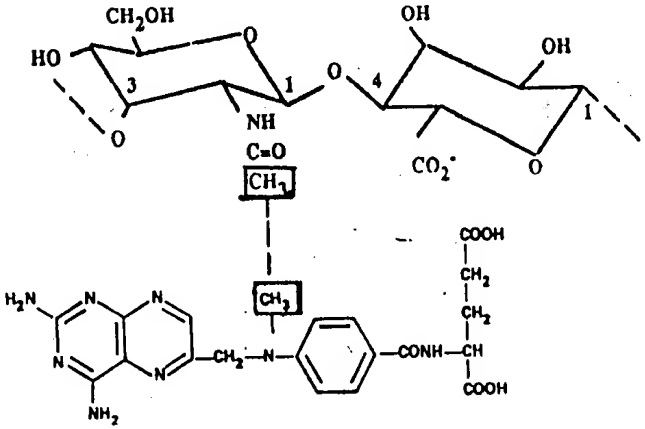

B: Entanglement of Methotrexate in Hyaluronan Molecule

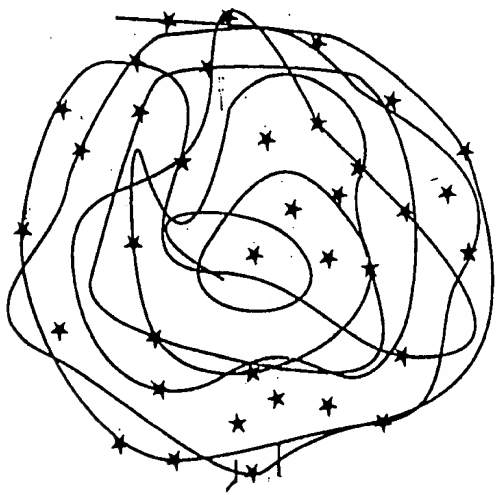

FIGURE 2

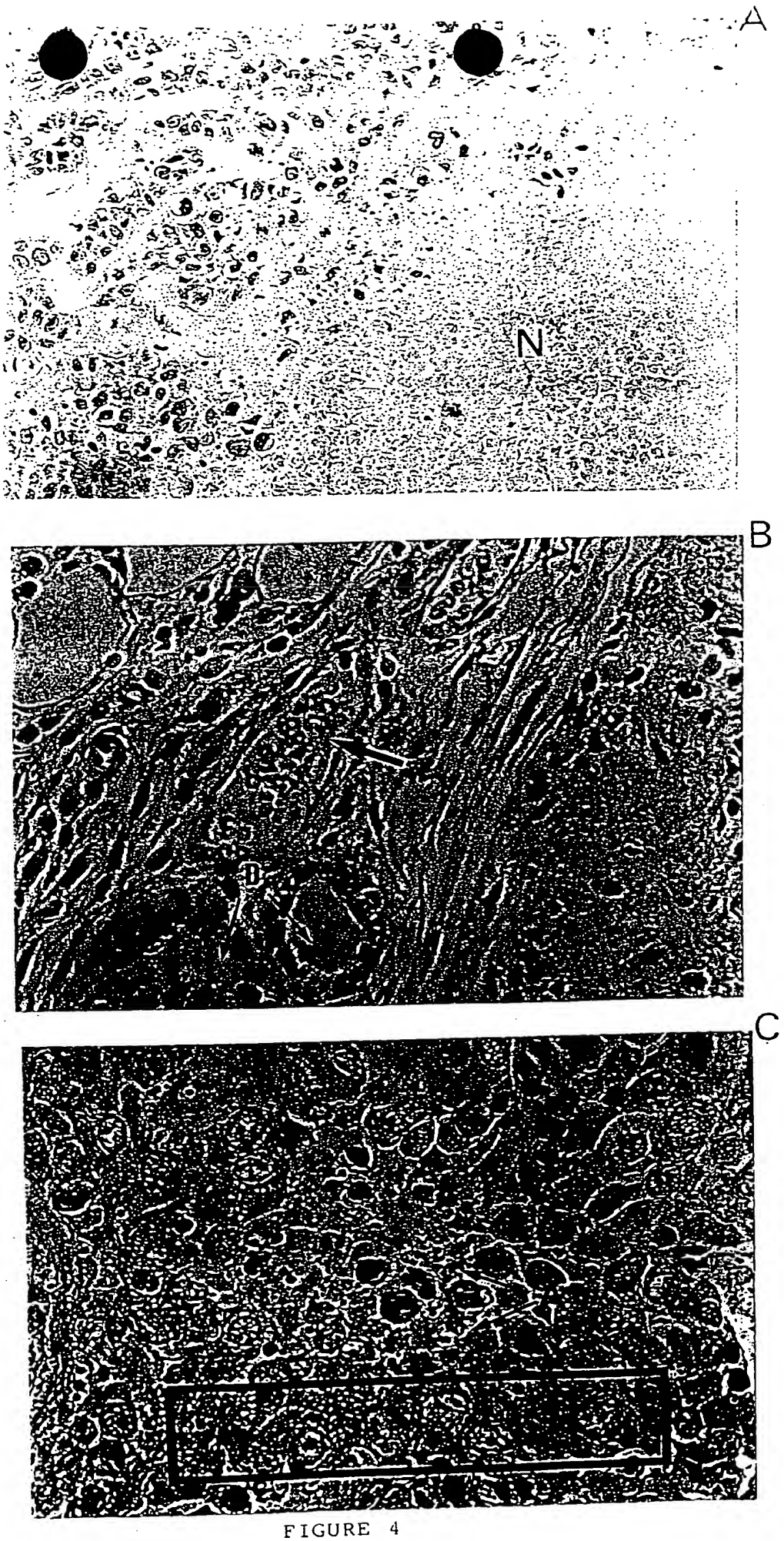

FIGURE 4

Molecular weight characterisation of hyaluronan used as a delivery vehicle for methotrexate

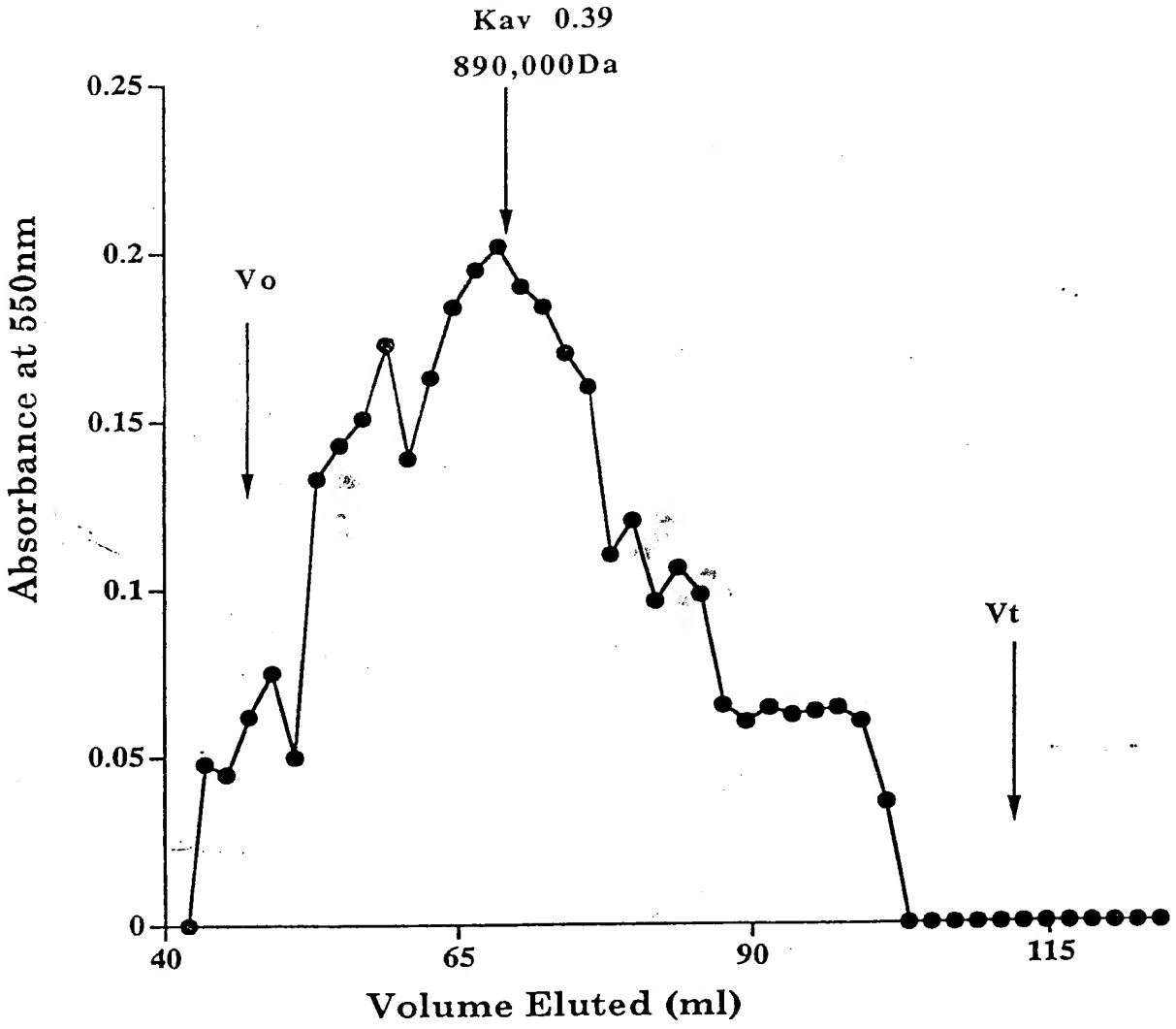

FIGURE 6

Increased methotrexate uptake by the liver when drug is co-administered with hyaluronan

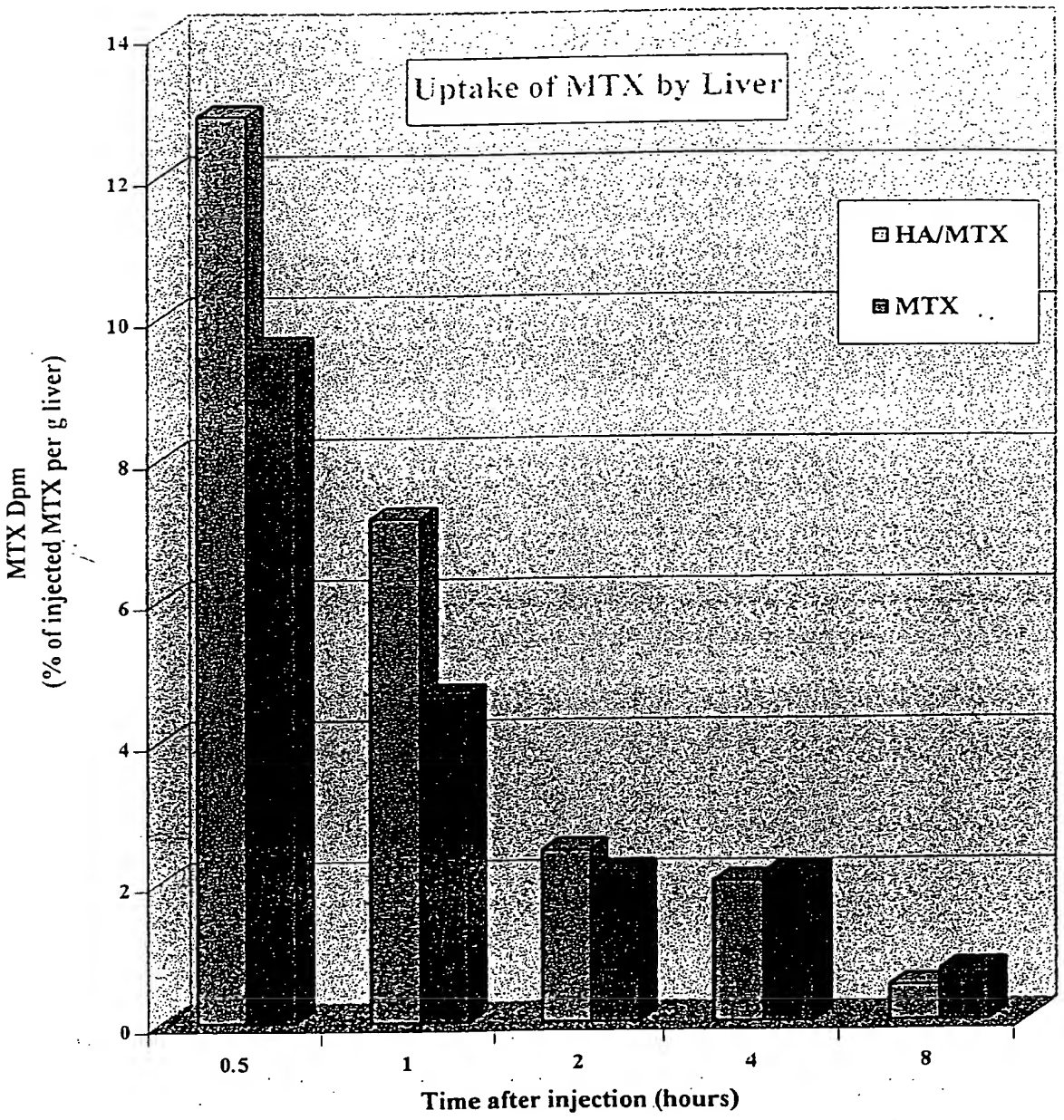

FIGURE 8

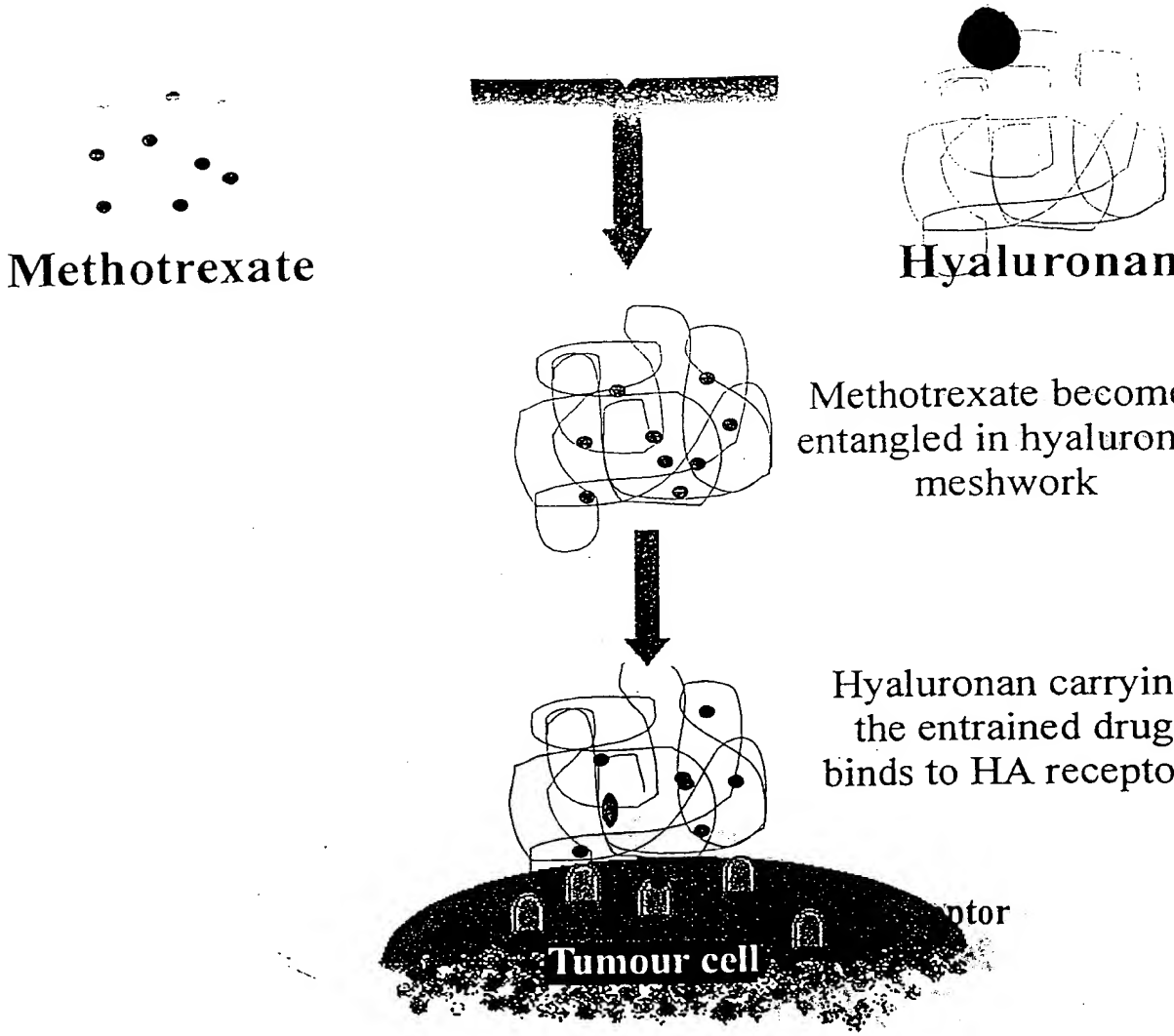

Two possible mechanisms of drug targeting of tumour cells

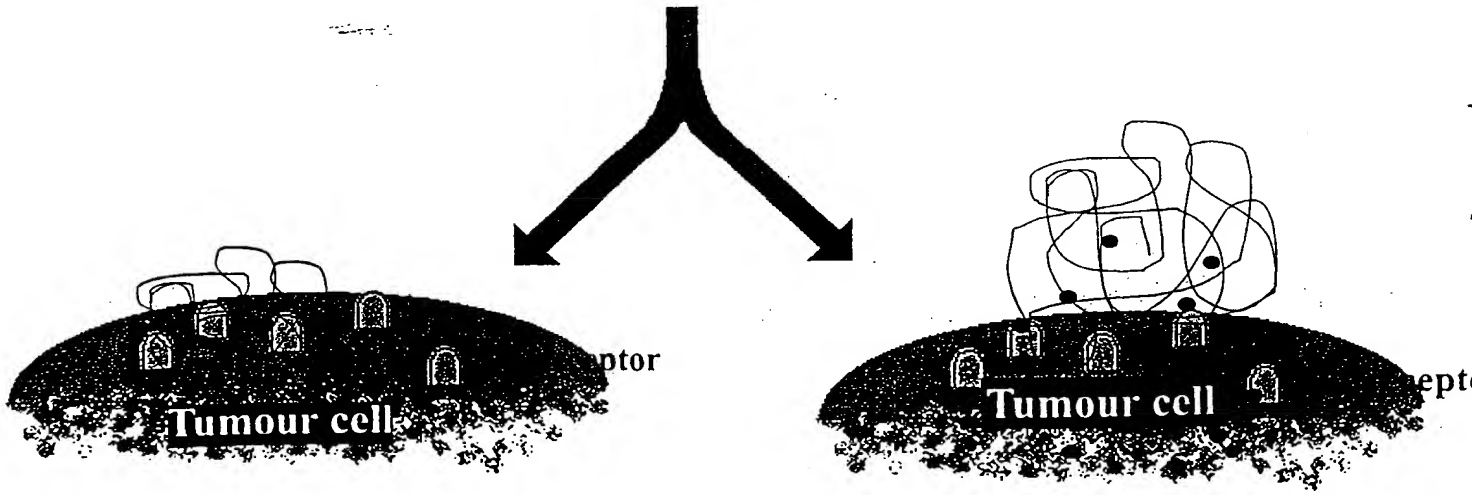

Possibility 1 - HA binds to the receptors and is internalised, so releasing drug into the tumour cell

Possibility 2 - HA binds to receptors, immobilising drug at tumour cell surface, enabling diffusion of drug into the cell or increased access to to drug internalisation mechanisms

FIGURE 10

Tumour Uptake of 5-Fluorouracil

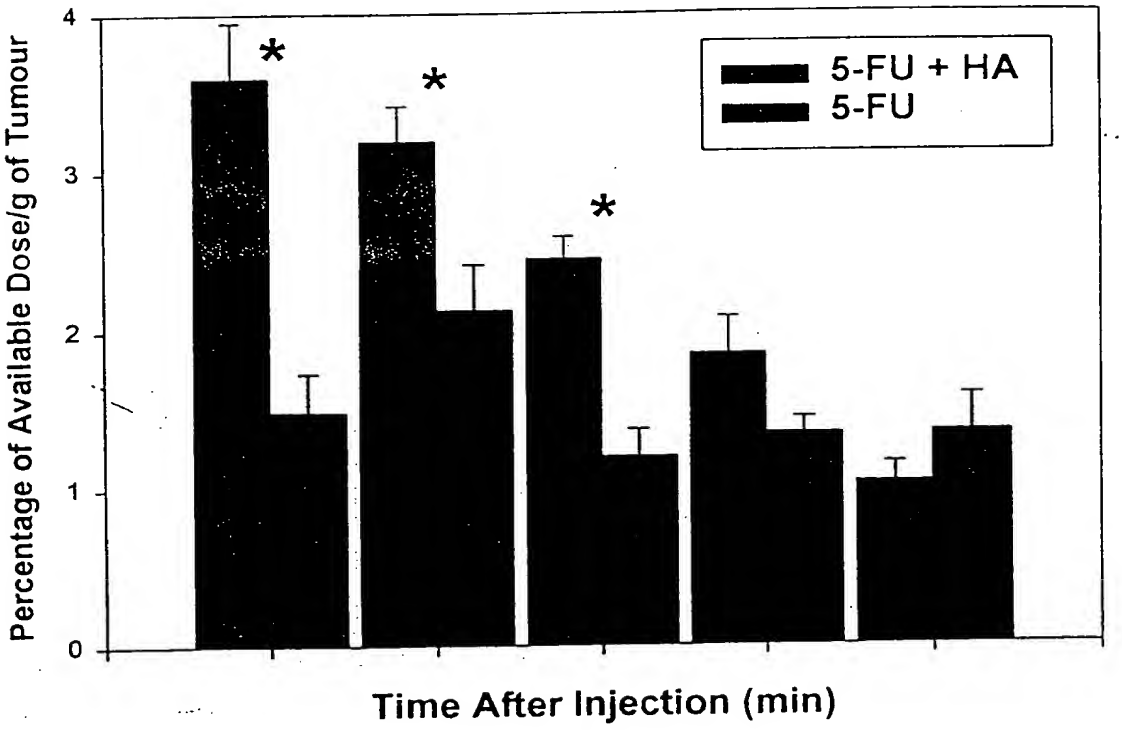

* P= or< 0.001, Students t-test

Figure 12

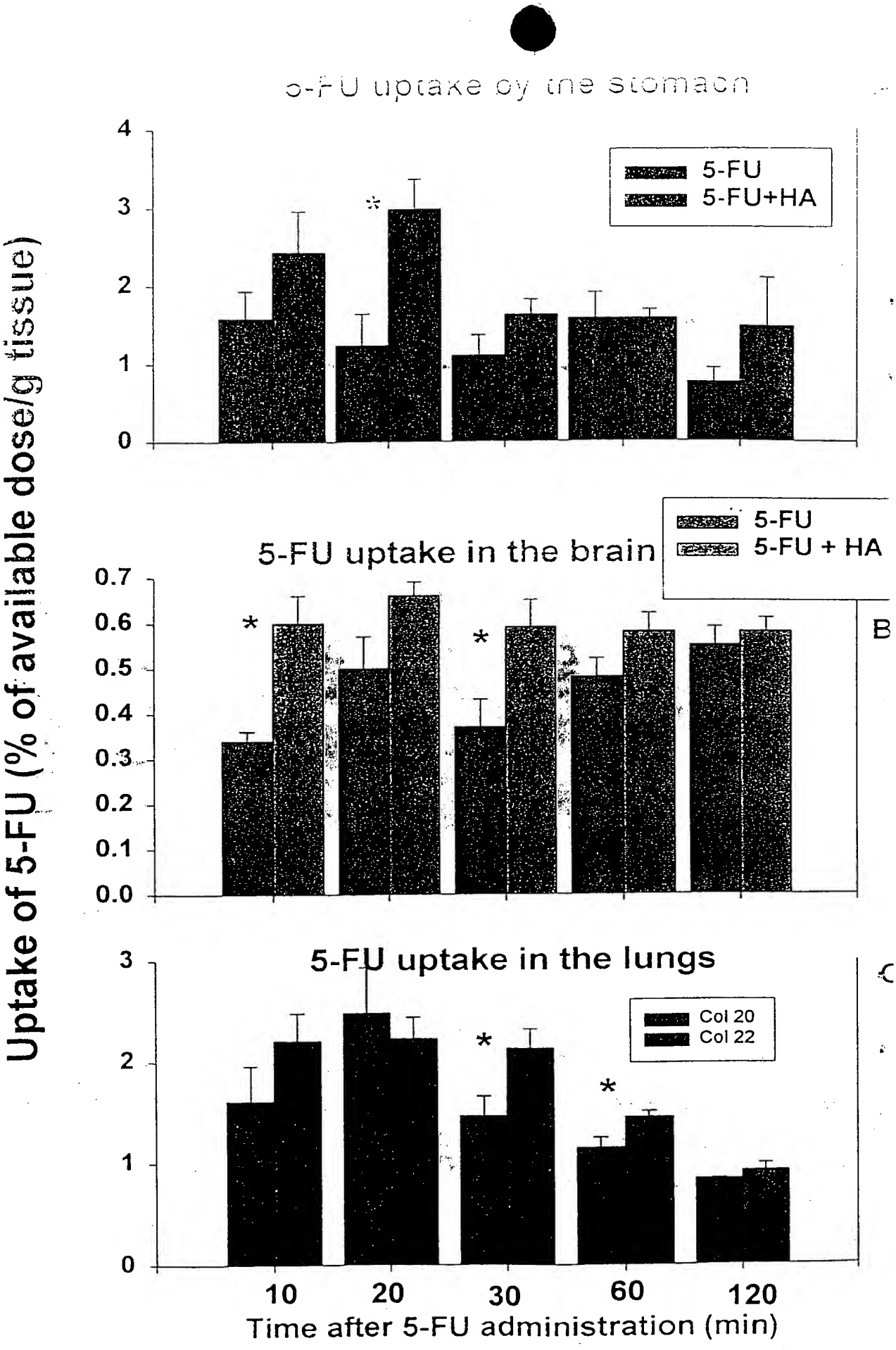
5-FU uptake by the stomach
5-FU
5-FU+HA
5-FU uptake in the brain
5-FU
5-FU + HA
5-FU uptake in the lungs
Col 20
Col 22
Uptake of 5-FU (% of available dose/g tissue)
Time after 5-FU administration (min)
10
20
30
60
120
B
C

Figure 14

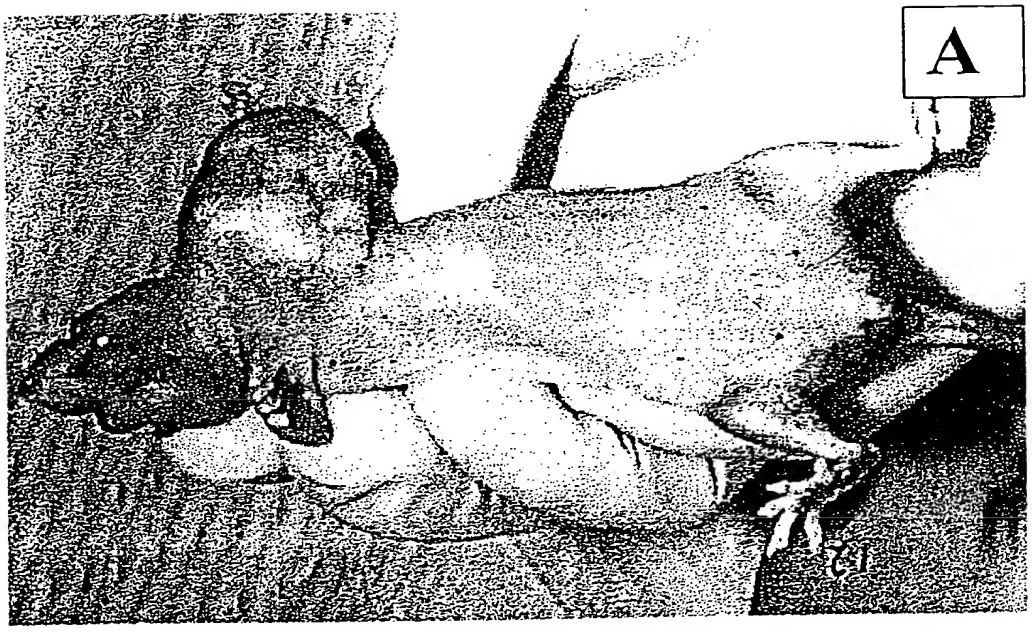

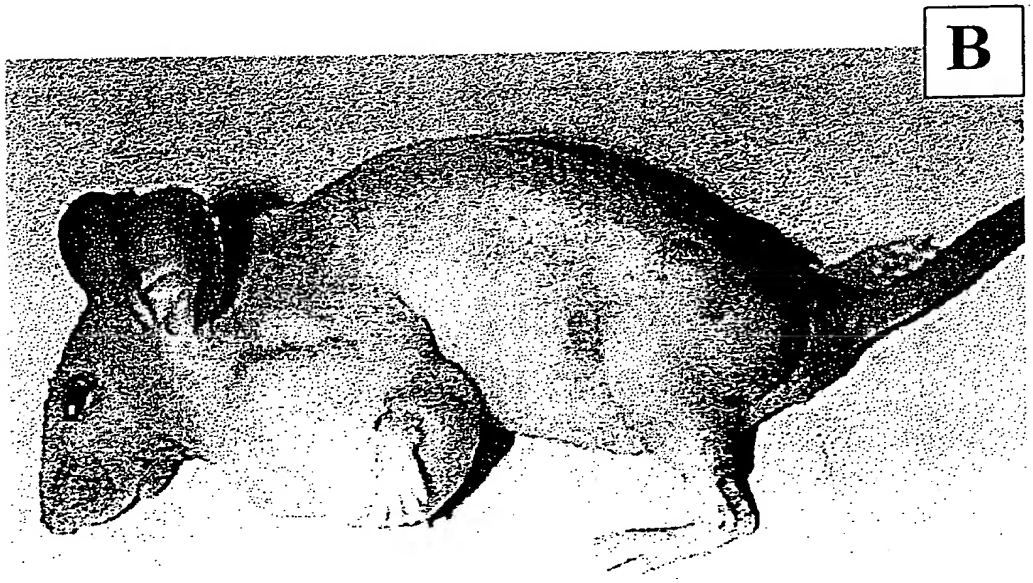

Figure 16

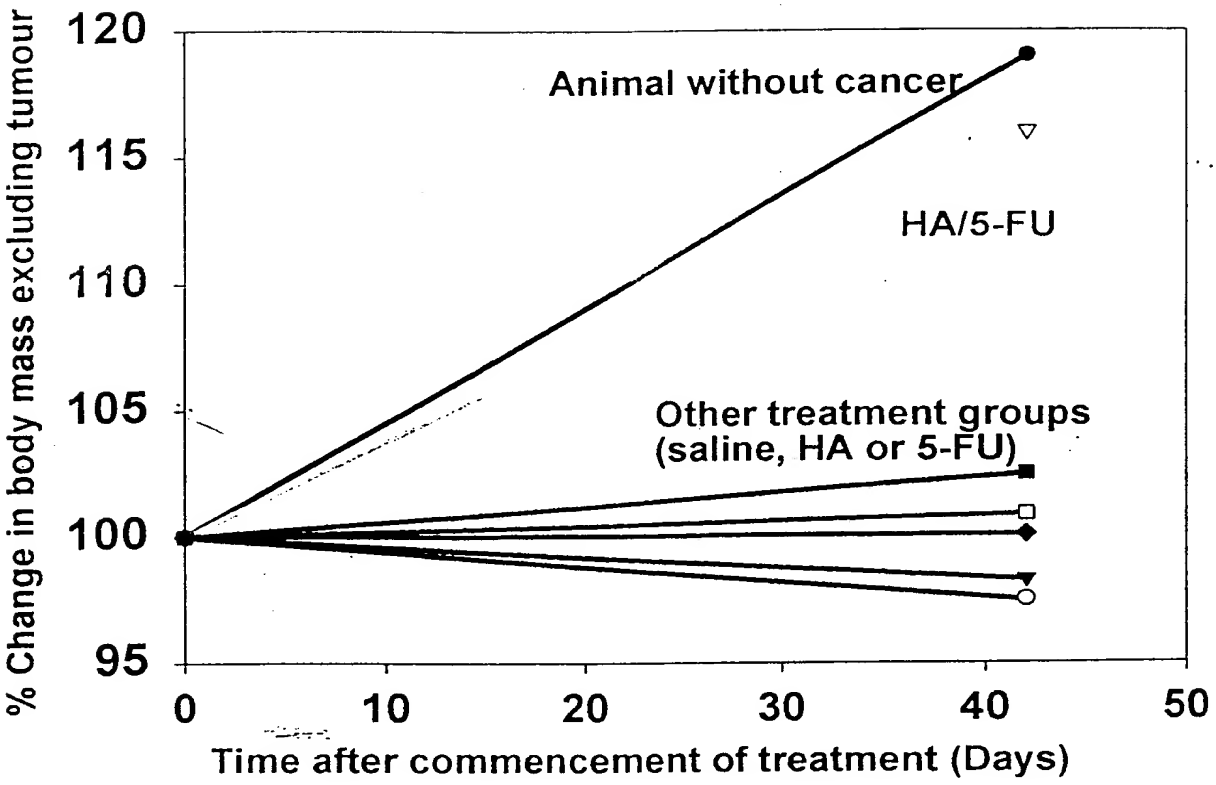
% Change in body mass excluding tumour
120
115
110
105
100
95
0
10
20
30
40
50
Time after commencement of treatment (Days)
Animal without cancer
HA/5-FU
Other treatment groups
(saline, HA or 5-FU)

Figure 18

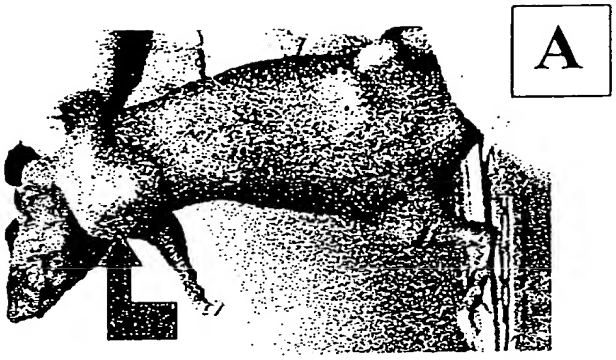

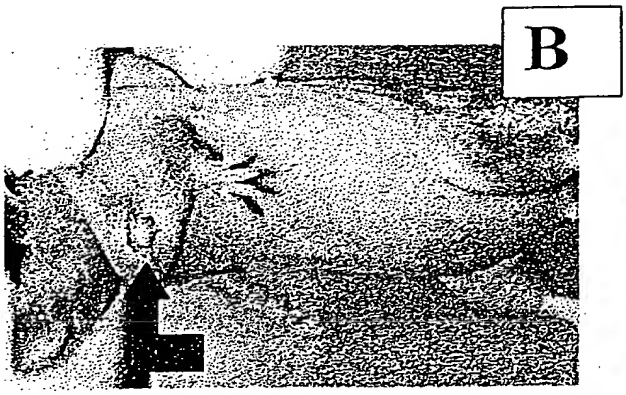

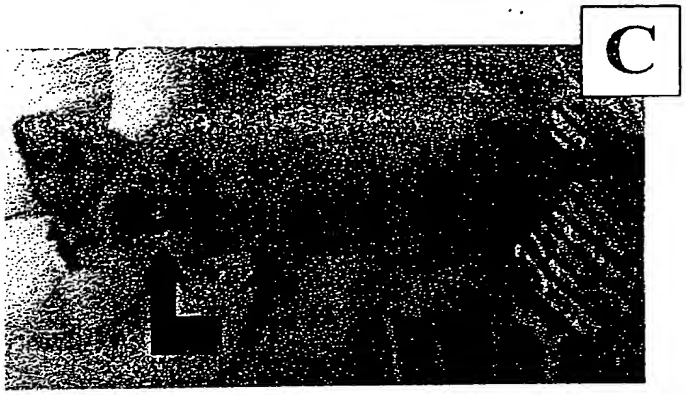

Figure 20